Springer

KSME

Journal of Mechanical Science and Technology 26 (1) (2012) 195~204
www.springerlink.com/content/1738-494x
DOI 10.1007/s12206-011-0938-2

Modeling of a hydraulic excavator based on bond graph method and its parameter estimation †

Soo-Jin Lee[1,*] and Pyung-Hun Chang[2]

[1] *Department of Mechanical Engineering, Myongji University, Yongin, 449-728, Korea*
[2] *Department of Robotics Engineering, Daegu Gyeongbuk Institute of Science and Technology, Daegu, 711-873, Korea*

(Manuscript Received November 26, 2010; Revised June 29, 2011; Accepted September 10, 2011)

Abstract

This paper focuses on two problems occurring in modeling a hydraulic excavator. The first problem arises in the modeling process. Because a hydraulic excavator has a very complex structure, the modeling process requires considerable time and is prone to errors. This problem is solved by conceptually modeling an excavator system using bond graph methods, the top-down and bottom-up methods, and the modeling software developed by the authors, and then, automatically deriving the nonlinear symbolic mathematical model from the conceptual model by using the modeling software. The other problem arises in obtaining parameters of the model. It is difficult to obtain the specification data for hydraulic components provided by manufacturers in general and to obtain the experimental data for estimating unique parameters. To solve this problem, an estimation method is devised for estimating parameters based on the experimental data that can be easily obtained. These methods enable easy and efficient modeling of an excavator system. In addition, the established model is verified through the comparison between the simulation and the experimental results. Also, this paper provides a good example of modeling of the large complex system.

Keywords: Bond graph modeling; Hydraulic excavator; Modeling software; Parameter estimation; Top-down and bottom-up modeling

1. Introduction

Owing to its ability to perform a large number of functions and its applicability to various types of situations, the hydraulic excavator is widely utilized among today's vast array of heavy construction equipment. Due to the ever-increasing size and complexity of construction sites, the demand for the hydraulic excavator is expected to continue to increase in the near future. However, contrary to this expected increase in equipment demand, the abundance of skilled operators is declining because it usually requires 3~5 years of handling experience to become a skilled excavator operator and the working conditions at construction sites are poor. To solve these problems, much research on automating excavator operations is being conducted [1-3]. In addition to automation of the hydraulic excavator, there is also research being conducted on its modeling. A dynamic model of the excavator can be used for development of an automation algorithm and the subsequent testing of this algorithm without incurring high costs [1, 4]. The model can also be applied to various situations such as simulation training for excavator operators [5] or estimation and analysis of systems' characteristics.

The following research has been conducted in relation to the modeling of the hydraulic excavator and other heavy hydraulic machinery similar to the hydraulic excavator. Yoshimura and Etokoro [4] modeled an excavator system and conducted simulation on the control of its manipulator. Papadopoulos et al. [6] used a linear graph to establish a model and conduct parameter estimation for the forestry machine which has a similar structure to that of an excavator. Li [7] modeled an electro-hydraulic mining manipulator using the methods investigated by de Pennington et al. and Handroos and Vilenius. The methods were applied to model the hydraulic components and Simulink was used for the simulation. Also, various methods were used to estimate each parameter of the hydraulic excavator. Kleinsteuber and Sepehri [8] used the polynomial abductive network modeling technique to model an excavator. In this research, calculation time of simulation was reduced by applying a high order polynomial functional relationship instead of using the exact functional relationship and parameter of the hydraulic system.

This paper deals with two problems concerning the modeling of an excavator system which previous research does not address. The first problem involves the complications arising

† This paper was recommended for publication in revised form by Associate Editor Moon Ki Kim

* Corresponding author. Tel.: +82 31 330 6345, Fax.: +82 31 321 4959
E-mail address: visionsj@mju.ac.kr

due to the complexity of the excavator system. Due to the complexity of the hydraulic circuit, which powers an excavator system, the modeling process consumes a great deal of time and there exists a large possibility of error. In addition, there exists the burden of having to repeat the modeling process every time a new model type is used. The second problem is estimating each parameter of the hydraulic system. It is difficult to obtain data that provides the exact parameter for each component within the hydraulic system. Consequently, each parameter must be obtained through either tuning or estimation. However, since a large number of parameters exist, obtaining parameters by tuning will require much effort and time. To apply the estimation method, the relevant experimental results that are required to determine each parameter must be provided. However, considering the structure of a hydraulic excavator system, it is very difficult to obtain all the necessary experimental results.

To solve the first problem, our research has been conducted applying a bond graph, top-down and bottom-up methods, a method that allows automatic derivation of a mathematical model in a nonlinear symbolic form, and modeling software developed by the authors to apply these methods. The following is a detailed explanation of our research. As is generally known, the bond graph [9] is used for graphic modeling of various types of systems. A systematic modeling method [10] using top-down and bottom-up, together with a bond graph enables us to easily and systematically model large complex systems like a hydraulic excavator. This method also allows easy identification and correction of errors during the modeling process. In the aforementioned software [10], modeling can be performed using the systematic method with bond graphs and a nonlinear symbolic mathematical model can be automatically obtained from an established model. By establishing a model through applying this method, modeling for the excavator not only becomes much easier and faster, but also when altering the model structure, only the altered parts need to be remodeled and then assembled. To deal with the second problem, our research proposes a method to estimate each parameter of the hydraulic system using only experimental results that are easily obtainable.

This paper is organized as follows. The introduction is presented in Section 1, and Section 2 details our excavator modeling process. The estimation process of each model parameter is presented in Section 3, while Section 4 presents the simulation results when applying the established model and parameters and compares them with the experiment results. And finally, in Section 5, the conclusion is presented.

2. Modeling of the excavator system

Fig. 1 shows the exterior of the hydraulic excavator that is to be modeled. The upper frame, which is rotated by a hydraulic motor, rests on the top of the lower frame, where the running device is located. The manipulator consisting of the boom, arm and bucket is also attached to the upper frame and

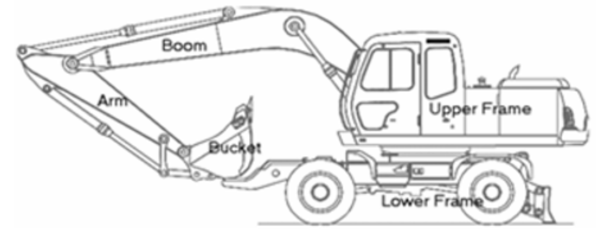

Fig. 1. Exterior of the hydraulic excavator [2].

is powered by hydraulic cylinders. This section details our efforts in modeling a hydraulic excavator by applying the bond graph and top-down/bottom-up methods while using modeling software developed by the authors.

2.1 Modeling

The top-down method initially divides a single system into several modules (subsystems) and then proceeds to further divide each module into lower level modules. During this process of division, the relation between each module must be clearly indicated. Since the bond graph method interprets the relation between each component on the basis of energy transmission, the relation between each module is presented in the energy-transmitting mode. The bottom-up method, an inverse method to the top-down method, analyzes each component within the system separately with each component forming a module. This method then combines the individual modules into a higher level module. While the top-down method is usually adopted when conducting modeling, if necessary, the bottom-up method is also adopted. For example, when it is difficult to determine the relation of a module with other modules, the relation between each module can be easily determined by closely examining the inner configurations of each module. For this case, it will be advantageous to adopt the bottom-up method for the modeling process. The interior of the bottom level module is presented by using symbols of the bond graph.

After having constructed a model by applying the top-down and bottom-up methods, the next stage is to rectify any problems concerning the model itself. This process is undertaken by applying the bottom-up method. We can examine the relations between each bottom level module on the basis of knowledge and understanding for the interior of the bottom level module. During this sequence, the identified problems are corrected, and by utilizing the information concerning the bottom level modules, verification and correction for modules at the next adjacent higher level is conducted. This process is iteratively conducted until the top level modules are affected. Thus, the top-down and bottom-up methods iteratively for further verification can enhance the reliability of the model [10].

Now consider modeling using the bond graph, the top-down and bottom-up methods, and the developed software. The scope of modeling will be limited to the boom, arm and bucket links, the relevant hydraulic actuator, and the energy

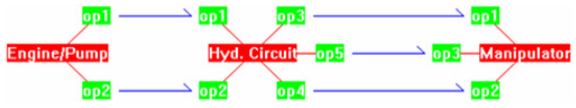

Fig. 2. Overall model of excavator.

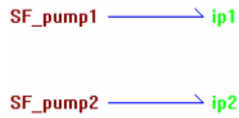

Fig. 3. Engine/pump module.

generating engine/pump. The manipulator consisting of only the boom, arm and bucket links performs important works such as straight motion tracking. With regards to this limited scope, the excavator can be divided into the modules - the engine/pump, hydraulic circuit, and the manipulator consisting boom, arm and bucket links. Fig. 2 depicts the modeling results if modeling for each part is conducted by applying the *Module Element* function of the software [10]. By observing this figure we can recognize that the Engine/Pump, Hyd. Circuit, and Manipulator are modules representing the engine/pump, hydraulic circuit and manipulator respectively. *op* refers to the port connected to the interior of the module while the number code is listed to indicate the matching port within the module. Because the generated energy from the two pumps is relayed to the hydraulic circuit, two bonds are used to connect the engine/pump module and hydraulic circuit module. Also, since the hydraulic circuit powers the boom, arm and bucket links, three bonds are placed between the hydraulic circuit module and manipulator module to denote the transfer of energy.

2.1.1 Engine/pump module

If we conduct modeling of the interior of the engine/pump module from the overall model presented in Fig. 2, we can obtain Fig. 3. The engine/pump module consists of one engine and two pumps. Assuming that the specific behavior of the engine and pump does not affect the overall behavior of the system, we model engine/pump module as two flow sources. A flow source is a term used at the bond graph and is denoted as *SF_pump* in the figure. *ip1* and *ip2* are internal ports that respectively connect to *op1* and *op2* of the module exterior.

2.1.2 Hydraulic circuit module

Fig. 4 presents a detailed diagram of the particular parts of the hydraulic circuit which are to be modeled. As seen in the figure, the dotted line separates the hydraulic circuit into three large parts. Each part represents hydraulic modules relevant to the respective boom, arm and bucket links. The energy transfer between each module is made possible by placing bonds like arrangement of pipes within the hydraulic circuit. Since the boom and arm hydraulic modules receive energy from the pumps, they are connected to ports linked with the en-

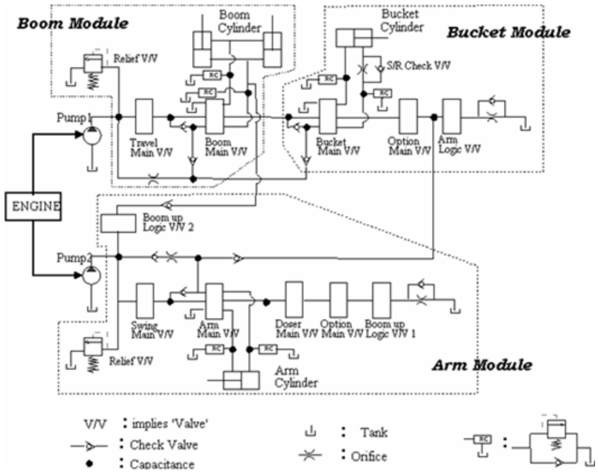

Fig. 4. Detailed map of the hydraulic circuit.

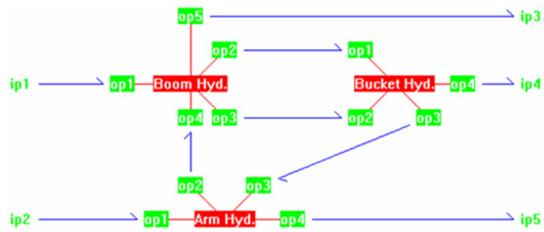

(a) Whole hydraulic circuit module

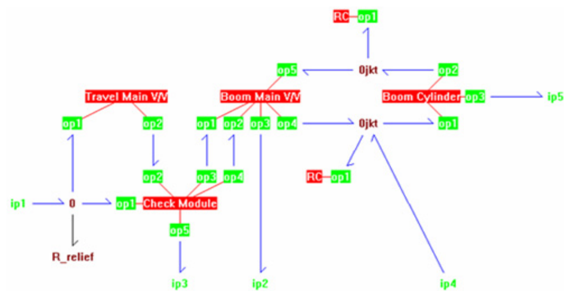

(b) Boom hyd. module

Fig. 5. Hydraulic module modeling.

gine/pump module. Also, since each cylinder within the boom, arm and bucket hydraulic modules connects to a corresponding link, each hydraulic module is connected to a port linked with the respective link module. The results of the modeling process stated above can be observed in Fig. 5(a).

Observing Fig. 5(a), the interior of each module is modeled in the same method that is used for modeling of Fig. 5(a). Modeling results for the boom hydraulic module are presented in Fig. 5(b). Finally, each component within the boom, arm and bucket hydraulic modules is modeled using the bond graph. Here, we will only consider modeling of the main valve, while the remaining parts will not be presented due to the page limit. The main valve possesses such a structure as observed in Fig. 6(a). If the joystick is at a neutral position as observed in the middle position of Fig. 6(a), the inflow and outflow

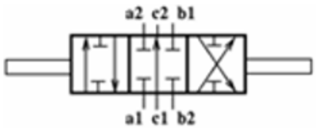

(a) Structure

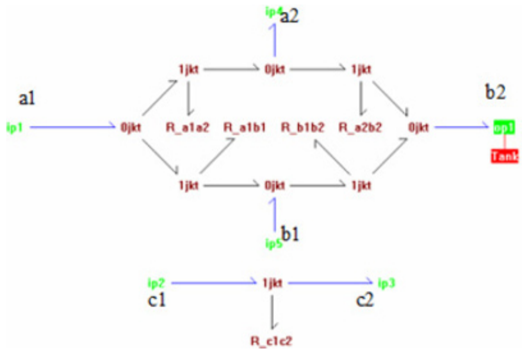

(b) Model expressed in bond graph

Fig. 6. Main valve.

ways (i.e., flow passages) of the valve leading to and from the cylinder become completely blocked, and the only way (c1-c2) remains open. The left/right positions in Fig. 6(a) represent instances where the joystick movement is present. For example, in the left position, the flow can be observed entering the cylinder through the (a1-a2) way and exiting through the (b1-b2) way. By modeling this structure applying the bond graph, we can obtain Fig. 6(b).

Although it does not appear to be visible, the *Capacitance* element plays an important role in the function of the hydraulic circuit. Because the fluid is compressible and the hydraulic pipes used for the transfer of fluid expandable, we must assume fluid compressibility and pipe expansion to be *Capacitance* elements and apply them properly when conducting modeling. Because each main valve and corresponding cylinder are linked together by a fairly long pipe, compressibility is highly evident in these parts. Consequently, we apply *Capacitance* elements to both ends of the cylinder (the 0 Junction connected to the RC Valve in Fig. 5(b)). *Capacitance* elements are inserted between pumps and main valves for the same reason [10].

2.1.3 Modeling of the manipulator

The coordinates for the manipulator are defined in Fig. 7. Because the energy transfer relationship between each link is not as clearly visible as that of the hydraulic circuit, it is preferable to apply the bottom-up method over the top-down one when conducting modeling. Also, when modeling a mechanical system using a bond graph, it is more suitable to conduct modeling based on *1 Junction* [9]. Consequently, the modeling process begins with determining the velocity of each link with *1 Junction* to form separate modules and then combining each module to form a higher level module.

Because the modeling processes for the boom, arm and bucket link modules are similar, only the arm link module will be discussed. The arm link performs rectilinear and rotational motion on a plane surface, so we can describe the motion using three velocities. Consequently, each velocity at the center of gravity is expressed as *1 Junction*. *1 Junction*, which represents the angular velocity, is connected to the *I* element, which represents the moment of inertia of the arm link at the center of gravity. Also, the torques acting on the *I* element are connected. The forces exerted on the *I* element are constraint forces occurring at joints connecting the arm link to the other links, forces generated from the arm and bucket cylinders, and gravitational force. The transformer (TF) converts each force into each torque, which is connected to *1 Junction*. This process of energy transfer is shown in Fig. 8(a), while in Fig. 8(b) the entire process is combined into a single module. Modeling the *1 Junctions* for the linear velocities in the directions of X and Y is omitted due to the page limit. By combining the three modules for the angular and linear velocities, we can obtain the interior of the Arm Link module as shown in Fig. 9. If

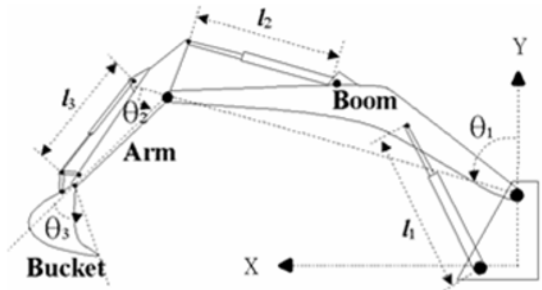

Fig. 7. Definition of the coordinates for links [2].

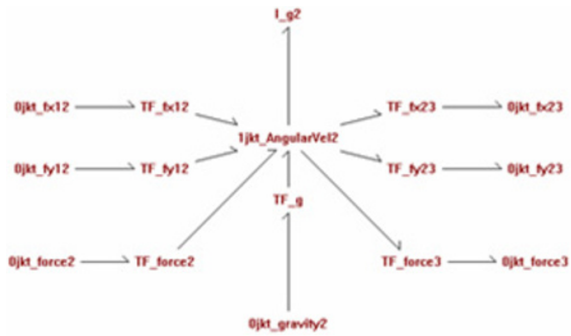

(a) Before modularizing

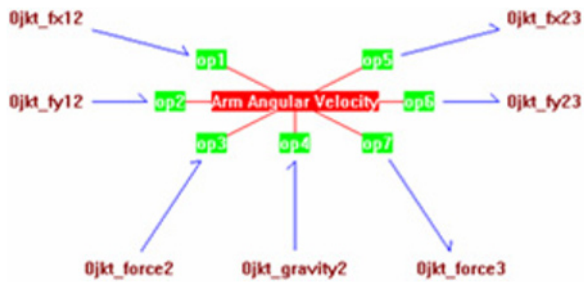

(b) After modularizing

Fig. 8. Model for the angular velocity of the arm link.

Fig. 9. Model of the arm link module interior.

Fig. 10. Modeling of the manipulator module.

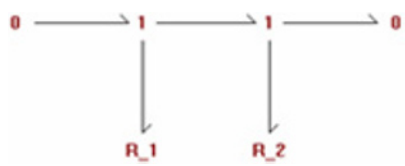

(a) Structure of two valves

(b) Combining two valves

Fig. 11. Boom up logic valve 2 and check valve.

connecting three link modules after the modules for three links have been constructed, the manipulator module in Fig. 2 is completed as in Fig. 10 [10].

2.1.4 Model revision

Now, the constructed model will be revised applying the bottom-up method. We can observe that the boom up logic valve 2 and check valve within the Arm Hyd. module featured in Fig. 5(a), are connected in the manner shown in Fig. 11(a). And during the examination for causality, we can observe that the causality of the two *R* (resistance) elements cannot be uniquely determined, which causes an algebraic loop making numerical calculation difficult. To solve this problem, resistances occurring at both the boom up logic valve 2 and check valve are combined into a single *R* element as shown in Fig. 11(b). This phenomenon also occurs between the doser main valve, option main valve, boom up logic valve 1, and foot relief valve located next to the boom up logic valve 1. Therefore, the four resistances are combined into a single resistance element. In other modules, this kind of modification is performed.

Because the length of the pipes connecting each main valve is short, the effect of compressibility is not high. However, to solve the problem of causality, we have included the *Capacitance* element expressed as the black circles in Fig. 4 where those at both cylinder ends and pump outlet are used to show the effect of capacitance itself.

To be more specific, the causality issue can be explained as follows. The valves, according to causality, are expressed as either one of the following two Eqs. [11]:

$$Q = c_q A\sqrt{|P_a - P_b|}, \tag{1}$$

$$P_a - P_b = \frac{Q^2}{(c_q A)^2} \tag{2}$$

where Q denotes the flow amount passing through the valves, and P_a and P_b are pressures at both ends of the valve. A is the cross-sectional area of the valve way, while c_q is the flow coefficient which includes the density of fluid. When the valve becomes shut, the cross-sectional area of the valve way, A, is zero, which makes numerical calculation in Eq. (2) impossible. Consequently, to express the opening and shutting of the valve, we must assign the valve the causality relevant to the form of Eq. (1) and this is made possible by including *Capacitance* element.

2.2 Creating a nonlinear symbolic mathematical model

After constructing a model as mentioned in section 2.1, we can automatically obtain a symbolic mathematical model by using the function of the software. After automatically assigning causality, we input the elemental equation of each element according to its own individual causality. And then by using the function, which allows for the automatic calculation of the mathematical model, we have obtained 20th order differential equations in a nonlinear symbolic form.

3. Parameter estimation

To accurately estimate the parameters of the hydraulic system of the excavator, we must measure the flow passing through each hydraulic component and the pressure level before and after fluid passes through the components. However, since all the main valves are located within the main control unit, it is impossible to measure the flow and pressure level required to estimate the parameter of each main valve. Therefore, in this section, we propose a method, using only minimum measurement data, for the estimation of each parameter. The measurement data of the hydraulic system enabling simple measurement are the pressure levels at both ends of the cylinders and both pump outlets. Also, the angles of the boom, arm and bucket links were measured.

The parameters for the hydraulic excavator can be classified into manipulator and hydraulic circuit parameters. Of these parameters, the individual mass, moment of inertia, and length of the boom, arm and bucket links all adopted values provided in the specification.

3.1 Flow coefficient

As expressed in Eq. (1), the relationship between the amount of flow (Q) passing through the hydraulic valve and the pressure difference (ΔP) at both ends of the valve is modeled as follows [11]:

$$Q = c_q A\sqrt{\Delta P}. \tag{3}$$

As observed in Eq. (3), the parameters that need to be measured at the valve are c_q and A. The value of A can either vary or remain constant, and in instances where the value of A varies, we used the data provided in the specification. While in instances where the value of A remains constant, we estimated the product of c_q and A.

As observed in Fig. 6(a), each main valve possesses several flow passages and the flow coefficients for the flow passages where fluid moves from the cylinder into the tank were estimated by using Eq. (3) where the flow amount (Q) was estimated in the following:

$$Q = Q_{pump}\frac{A_{out}}{A_{in}} \tag{4}$$

where Q_{pump} denotes the flow amount of the pump; A_{in} is the area of the piston at the inflow side of the cylinder and A_{out} is the area of the piston at the outflow side of the cylinder.

The flow amount of the pump is estimated by using the pressure level at the pump outlet and the provided pressure-flow curve of the pump. ΔP is the difference between the pressures at the outflow side of the cylinder and the tank. The pressure level at the outflow side of the cylinder was measured while the tank pressure was assumed to be the same as the atmospheric pressure.

Since the foot relief valve located next to the arm logic valve and boom up logic valve 1 in Fig. 4 consists of the check valve and orifice, the flow coefficient for the valve is the sum of the separate flow coefficients of the check valve and orifice. This can be estimated by using the following equation:

$$c_{qA} = \frac{Q}{\sqrt{\Delta P}} \tag{5}$$

where Q and ΔP are provided in the specification, and c_{qA} means the product of flow coefficient and area of valve.

When the main valve of the arm is completely open and the other main valves completely shut, the flow path between two pumps and the arm cylinder can be expressed using equivalent flow coefficients ($Ceq1$, $Ceq2$) and the flow coefficient of the arm valve ($Cq3$) as shown in Fig. 12.

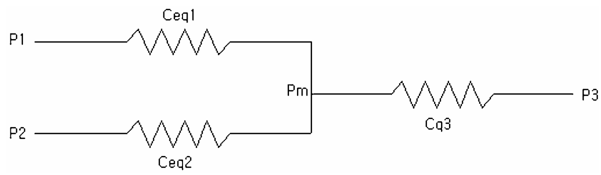

Fig. 12. Flow path between the two pumps and the arm cylinder.

In Fig. 12, $P1$ and $P2$ denote pump pressures, $P3$, the pressure at the inflow side of the cylinder, and Pm is the pressure level right before the flow enters the main valve. From Fig. 12, we can obtain the following flow equations:

$$\begin{aligned}
&Q1_{in} = Ceq1\sqrt{P1_{in} - Pm_{in}}, \\
&Q1_{out} = Ceq1\sqrt{P1_{out} - Pm_{out}}, \\
&Q2_{in} = Ceq2\sqrt{P2_{in} - Pm_{in}}, \\
&Q2_{out} = Ceq2\sqrt{P2_{out} - Pm_{out}}, \\
&Q3_{in} = Cq3_{in}\sqrt{Pm_{in} - P3_{in}}, \\
&Q3_{out} = Cq3_{out}\sqrt{Pm_{out} - P3_{out}}
\end{aligned} \tag{6}$$

where the subscripts *in* and *out* denote when the arm is either folded or spread. $Q1$ and $Q2$ denote the flow amount of the respective pumps and $Q3$ is the sum of $Q1$ and $Q2$.

The flow coefficients ($Ceq1$, $Ceq2$, $Cq3_{in}$, $Cq3_{out}$) and pressures (Pm_{in}, Pm_{out}) are unknown quantities and can be estimated by using Eq. (6).

From Fig. 4, we can observe that between $P1$ and Pm, the bypass ways of the travel main valve, boom main valve, bucket main valve, and option main valve are serially linked. Consequently, $Ceq1$ is an equivalent flow coefficient to flow coefficients of these four valves. By assuming that the four flow coefficients are identical, each (c_{qA_b}) is estimated by using the following relationship:

$$c_{qA\_b} = 2Ceq1. \tag{7}$$

Between $P2$ and Pm, the orifice and the bypass way of the swing main valve are parallel linked and $Ceq2$ is also the equivalent flow coefficient of these two flow coefficients. Since the maximum area of the bypass way in the swing main valve is less than the maximum areas of bypass ways in the other valves, we can estimate the flow coefficient of the bypass way in the swing main valve, c_{qA_swing}, by using the area ratio while the flow coefficient of the orifice is estimated by using the following equation:

$$c_{qA\_ori} = Ceq2 - c_{qA\_swing}. \tag{8}$$

$Cq3_{in}$ and $Cq3_{out}$ represent the flow coefficients of passages in the arm main valve leading from the pump into the cylinder when the arm is either folded or spread.

There are many check valves included in the flow passages of Fig. 12. However, because a check valve is used to either open or shut a flow passage and its resistance level considera-

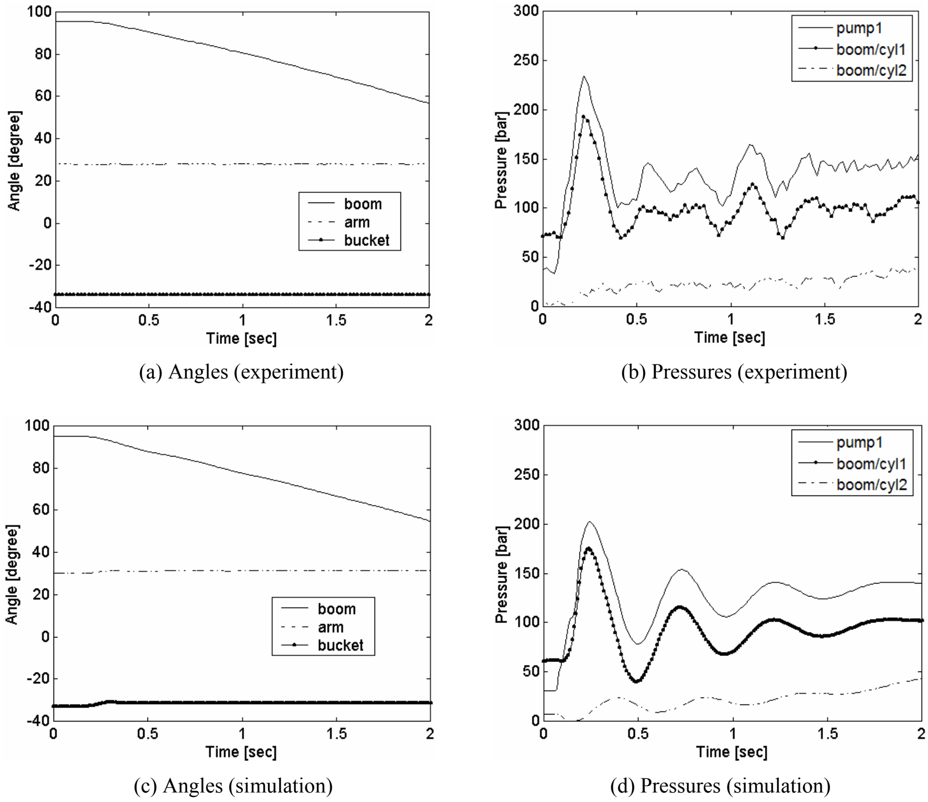

(a) Angles (experiment) (b) Pressures (experiment)

(c) Angles (simulation) (d) Pressures (simulation)

Fig. 13. Boom motion.

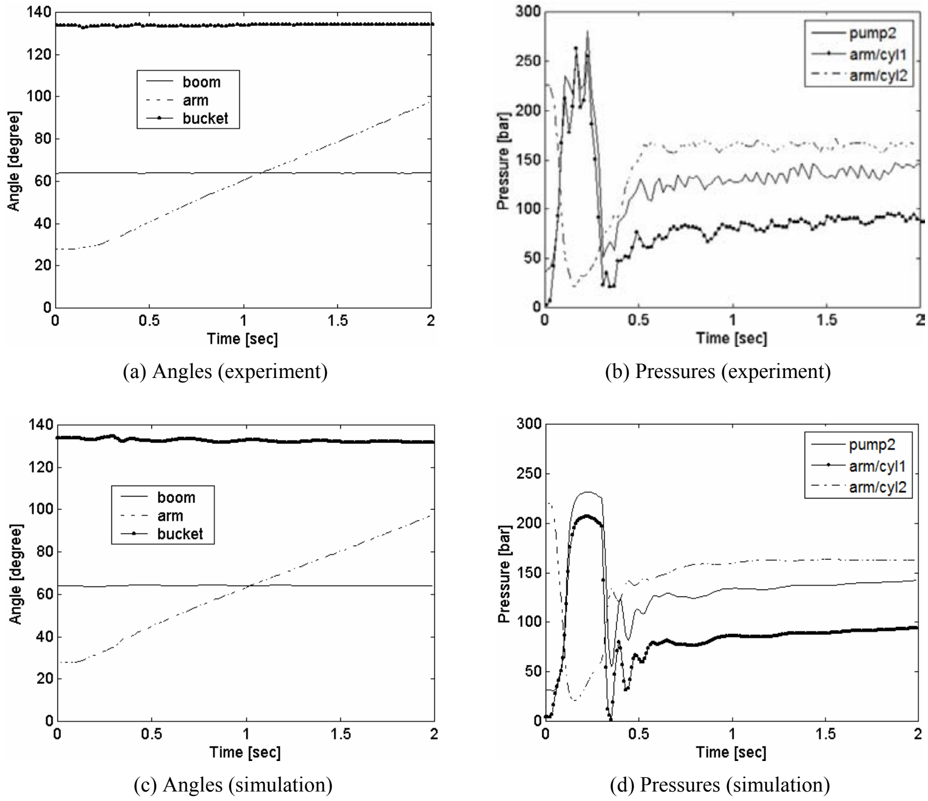

(a) Angles (experiment) (b) Pressures (experiment)

(c) Angles (simulation) (d) Pressures (simulation)

Fig. 14. Arm motion.

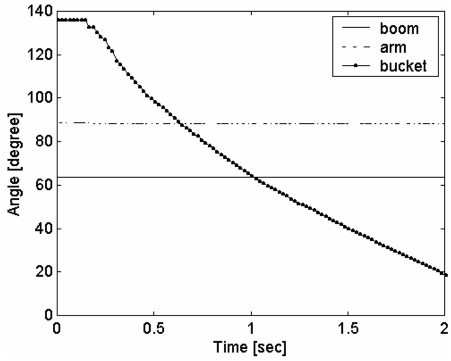

(a) Angle (experiment)

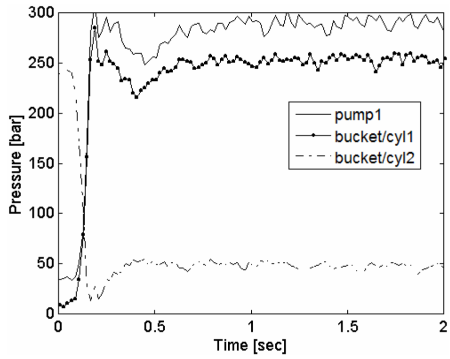

(b) Pressures (experiment)

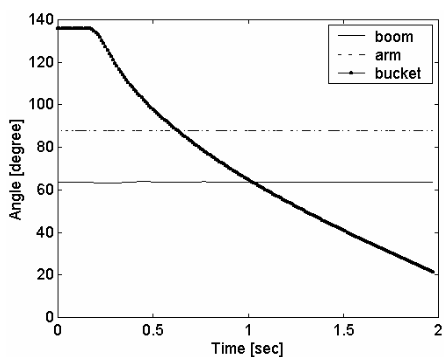

(c) Angles (simulation)

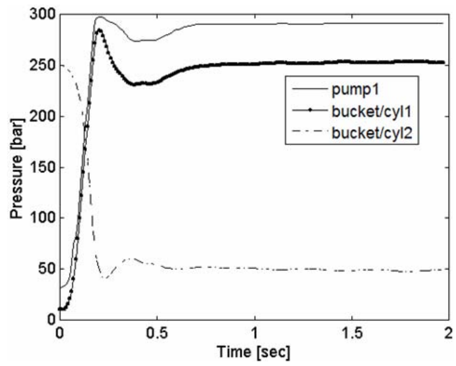

(d) Pressures (simulation)

Fig. 15. Bucket motion.

bly less than that of other valves, we have not included them in the equivalent resistances shown in Fig. 12. In addition, the flow coefficients of the check valves were adjusted so that resistance level was considerably less than that of other valves.

In instances where flow is generated by the opening of the boom main valve or bucket main valve, the flow coefficients related to the generated flow were estimated in a similar method to that for the arm. In addition to these cases, there are the following flow coefficients. The flow coefficients of the bypass ways of the arm main valve, option main valve, and doser main valve within the arm hydraulic module were adjusted so that they retained identical values to the bypass way coefficients of other main valves.

3.2 Capacitance coefficient

If the main valve is shut, thus resulting in the isolation of flow inside the cylinder, each link vibrates in the following manner:

$$M\ddot{\theta} + K\theta = residue \tag{9}$$

where θ denotes the angle of each link, and M and K the inertia and stiffness coefficient of each link. The stiffness coefficient is derived as follows:

$$K(\theta) = \beta_0 \left(\frac{A_{cyl1}^2}{V_{cyl1}(\theta)} + \frac{A_{cyl2}^2}{V_{cyl2}(\theta)} \right) \tag{10}$$

where $V_{cyl1}(\theta)$ and $V_{cyl2}(\theta)$ denote the volume of fluid inside both chambers of the cylinder and the relevant pipes from the main valve to the cylinder, and β_0 is the bulk modulus of the fluid.

Using the measured angle trajectory of each link, the natural frequency of the system expressed as Eq. (9), ω_n is calculated and the stiffness coefficient, $K(\theta)$, is obtained from the following:

$$K(\theta) = \omega_n^2 M(\theta). \tag{11}$$

After estimating the bulk modulus by using Eqs. (10) and (11), the capacitance coefficient, C_*, can be obtained from the following:

$$C_* = \frac{V_*}{\beta_0}. \tag{12}$$

There are capacitances added to solve the problem of causality. Owing to the rather short length of the hydraulic pipe relative to the capacitances, there is no mention of it in the specification. In this case, because the liquid volume was impossible to calculate, the adopted coefficient was adjusted to be significantly less value than the other capacitance coefficients.

4. Simulation and experiment for validation

In this section, we will conduct simulation using the previously constructed model and parameters, and compare the simulation results with the experiment results. The excavator which is used in the simulation and experiment is Hyundai HX60W-2 with the following specifications: the total weight is 13 tons and the bucket capacitance is 60 liters; the total length of the boom, arm and bucket is 7.55 m. For the generation of motion in the simulation and experiment, a maximum level of step input has been applied to the boom, arm and bucket main valves. Due to a time delay when applying input, the first order dynamics is added to the valve model.

Fig. 13 shows the experiment and simulation results when a maximum level of step input is applied to the boom main valve. We can observe that the movement angles of the boom link in both Fig. 13(a) and (c) are nearly identical. Fig. 13(b) and (d) indicate pressure levels at the pump outlet and at both sides of the cylinder. Comparing the pressure levels, we can observe that they are similar. The arm and bucket responses are shown in Fig. 14 and Fig. 15, respectively. We can observe that the responding angles of the arm and bucket links are similar throughout the course of the simulation and experiment. Also, there is a tendency for the pressure responses to be similar.

Observing the pressure responses, we can notice that there is a large amount of change in the early stages, but as the experiment reaches the latter stages, responses seem to be of steady state. Since the flow coefficients are estimated on the basis of the near steady state responses, there arise instances where the flow coefficients do not reflect the pressure changes that occur in the early stages of the experiment. In cases where this situation occurred, different flow coefficient values were used for the pressure responses in the early and latter stages.

5. Conclusions

This paper has focused on providing solutions to two problems that occur during the modeling of the hydraulic excavator. One problem is that the modeling process is difficult and is prone to errors due to the complexity of the excavator system itself. To solve this problem, the bond graph method, the top-down and bottom-up methods, and modeling software developed by the authors have been applied. By applying these methods to model the excavator system, we were able to simplify and adopt a more systematic approach to the modeling process. Also, the constructed model possesses the advantage that when the excavator structure is altered, model modification is necessary for only the altered components of the entire system. And because a relevant nonlinear mathematical model is automatically produced from the constructed hierarchical bond graph model, the difficulty associated with obtaining a model equation has been eliminated and errors occurring from deriving such a complex mathematical model have been reduced. These methods also enable the generation of equations in the symbolic form, which in turn becomes helpful when there arises situations where symbolic form is required.

To solve the other problem that occurs during the modeling of the excavator system, which is the difficulty of parameter estimation, we have proposed a parameter estimation method that is suitable with the hydraulic excavator. We only use data that are easily measured to estimate the parameters. This can solve the burden of having to conduct tuning by the trial and error method.

After having conducted the simulation, we compared the model responses with the experiment results. And we verified that angle and pressure responses in the simulation were similar to the experiment results. This paper presents the practical application of bond graph modeling to large complex multi-domain systems.

Acknowledgment

We gratefully acknowledge that a part of this research was done at DGIST with internal research fund.

References

[1] N. Sepehri, P. D. Lawrence, F. Sassani and R. Frenette, Resolved-mode teleoperated control of heavy-duty hydraulic machines, *ASME Journal of Dynamic System, Measurement and Control*, 116 (2) (1994) 232-240.

[2] P. H. Chang and S. J. Lee, A straight-line motion tracking control of hydraulic excavator system, *Mechatronics*, 12 (1) (2002) 119-138.

[3] L. D. Hanh, K. K. Ahn, B. B. Kha and W. K. Jo, Trajectory control of electro-hydraulic excavator using fuzzy self tuning algorithm with neural network, *Journal of Mechanical Science and Technology*, 23 (1) (2009) 149-160.

[4] T. Yoshimura and K. Etokoro, A Simulation study of leveling control by hydraulic shovels, *Transactions of the Japan Society of Mechanical Engineers Part C*, 58 (554) (1992) 161-167 (In Japanese).

[5] Y. Gonthier and E. Papadopoulos, On the development of a real-time simulator for an electro-hydraulic forestry machine, *Proc. of the IEEE International Conference on Robotics and Automation* (1998) 127-132.

[6] E. Papadopoulos, B. Mu and R. Frenette, Modeling and identification of an electrohydraulic articulated forestry machine, *Proc. of the IEEE International Conference on Robotics and Automation* (1997) 60-65.

[7] Z. D. Li, Modeling and simulation of an electro-hydraulic mining manipulator, *Proc. of the IEEE International Conference on Robotics and Automation* (1997) 1663-1668.

[8] S. Kleinsteuber and N. Sepehri, A polynomial network modeling approach to a class of large-scale hydraulic systems, *Computers and Electrical Engineering*, 22 (2) (1996) 151-168.

[9] D. C. Karnopp, D. L. Margolis and R. C. Rosenberg, *System Dynamics: A Unified Approach,* Second Ed. John Wiley & Sons, New York, USA (1990).

[10] S. J. Lee, Development and Application of a modeling method and software based on bond graph for large complex systems, *Korea Advanced Institute of Science and Technology, Ph.D. Dissertation* (2001) (in Korean).

[11] J. Watton, *Fluid Power Systems*, Prentice Hall International Ltd, UK (1989).

Soo-Jin Lee received his M.S. degree in Precision Engineering and Mechatronics, and the Ph.D degree in Mechanical Engineering from Korea Advanced Institute of Science and Technology (KAIST), Daejon, Korea. He was a Senior Research Engineer at the technical center of Hyundai Mobis belonging to Hyundai-Kia Automotive Group, Korea. He is now a member of the faculty of the Department of Mechanical Engineering, Myongji University, Yongin, Korea, where he is currently an Assistant Professor. His research interests include system dynamics, robust control of nonlinear system, vehicle simulator, and intelligent vehicle control.

Pyung-Hun Chang received M.Sc and Ph.D degrees both in Mechanical Engineering from Massachusetts Institute of Technology, in 1984 and 1987, respectively. He had been a professor at KAIST, Daejon, Korea for 24 years, and now is a professor and head of Robotics Engineering of DGIST, Daegu, Korea. His current research interests include rehabilitation robotics, robust control of nonlinear systems including kinematically redundant manipulators, and impedance control of dual-arm manipulators. He has authored more than 46 papers in international journals, 22 papers in domestic journals, and 88 papers in conference proceedings. Currently, he serves as the Dean of graduate studies of DGIST.